CLM-P603

CLM-P603

UKAEA

Preprint

DESTABILISATION OF DRIFT-UNIVERSAL EIGENMODES BY TOROIDAL EFFECTS

K. W. HESKETH

CULHAM LABORATORY
Abingdon Oxfordshire

1980

CLM-P 603

DESTABILISATION OF DRIFT-UNIVERSAL EIGENMODES BY TOROIDAL EFFECTS

K.W. Hesketh

Culham Laboratory, Abingdon, Oxon., OX14 3DB, UK

(Euratom/UKAEA Fusion Association)

ABSTRACT

An eigenvalue equation representing the drift-universal instability in toroidal geometry is investigated numerically. It is demonstrated that the form of passing electron Landau resonance appropriate to toroidal geometry can destabilise the slab drift wave.

(Submitted for publication in Nuclear Fusion)

January 1980

1. INTRODUCTION

It is now well established [1, 2] that, in a slab geometry with magnetic shear, drift wave eigenmodes in the absence of parallel current are always stable. In part, this is attributable to the stabilising influence of shear-induced damping. A recent investigation [3] using the Ballooning representation [4], has shown that this stabilising mechanism can be reduced by toroidal effects, such as ion curvature drift and $\underline{\nabla}B$ drift. These effects induce a coupling between Fourier modes centred on different rational surfaces and inhibit the outward convection of energy which is responsible for shear damping.

However, in reference [3] the question of the stability of drift waves in toroidal geometry is left unresolved, because a realistic form of the destabilising electron Landau resonance was not included. More recently [5] it has been shown how such effects can be incorporated within the Ballooning representation. The result is an integro-differential eigenvalue equation.

In the present work this equation is solved numerically. The essential result is that with suffiently toroidicity, absolutely unstable eigenmodes are found, driven by the electron Landau resonance. The effect of other parameters on these unstable eigenvalues is also investigated.

2. THE EIGENMODE EQUATION FOR DRIFT WAVES IN TOROIDAL GEOMETRY

In reference [5] details are given of the derivation of the eigenvalue equation for drift waves in toroidal geometry. Essentially this involves application of the Ballooning transformation to the Vlasov equation for the perturbed distribution functions of ions and electrons.

The problem is thereby transformed into a domain in which the poloidal variable η extends over an infinite range and into which the poloidal periodicity constraint does not enter. Solutions of the Vlasov equation in this domain lead to electron and ion responses which simplify considerably in the appropriate limit $\omega_i \ll \omega \ll \omega_e$ (where ω_i and ω_e are the electron and ion transit frequencies) and the equation becomes a one-dimensional integro-differential eigenvalue equation on each flux surface.

In the present paper we specialise to long wavelength drift modes in a large aspect ratio Tokamak, with circular magnetic surfaces, and retain only the passing electron contribution to the non-adiabatic part of the electron charge density. The eigenvalue equation is then given by

$$\frac{d^2\phi}{d\eta^2} + [\lambda - U(\eta)]\phi - i\beta\int_{-\infty}^{\infty} K(\eta,\ \eta')\ \phi(\eta')\ d\eta' = 0 \qquad (1)$$

where

$$\lambda = \left(\frac{\omega}{\omega_*}\frac{ka_i\tau}{\varepsilon_c}\right)^2\left[k^2a_i^2 - \frac{\omega_* - \omega}{\omega_* + \omega\tau}\right] \qquad (2)$$

$$U(\eta) = -\sigma^2\left[\eta^2 + 2\alpha\left(\cos(\eta + \eta_o) + S\eta\sin(\eta + \eta_o)\right)\right] \qquad (3)$$

$$\beta = \frac{1}{2\sqrt{\pi}}\left(\frac{\omega Rq}{v_{Te}}\right)\frac{\omega_*(1 - \eta_e/2) - \omega}{\omega_* + \omega\tau}\left(\frac{\omega}{\omega_*}\frac{ka_i\tau}{\varepsilon_c}\right)^2 \qquad (4)$$

$$\sigma \equiv \frac{\omega}{\omega_*}\frac{k^2a_i^2 S\tau}{\varepsilon_c},\qquad \alpha \equiv \frac{\varepsilon_n}{k^2a_i^2 S\tau}\frac{\omega_*}{\omega},\qquad S = \frac{rq'}{q},\quad \varepsilon_n = \frac{r_n}{R},\quad \varepsilon_c = \frac{r_n}{Rq},$$

$$v_{Te} = (2T_e/m_e)^{\frac{1}{2}},\quad \tau = T_e/T_i,\quad r_n^{-1} = n^{-1}(dn/dr),$$

$$\eta_e = \frac{1}{T_e}\frac{dT_e}{dr}\bigg/\frac{1}{n}\frac{dn}{dr},\qquad \omega_* = \frac{kT_e}{eBr_n},\qquad a_i = \sqrt{\frac{T_i}{m_i\,\omega_{ci}^2}},$$

$k = \ell q/r$, with ℓ the toroidal mode number and

$$K(\eta, \eta') = \ell n \left(\frac{2R}{r}\right) - 2 \ell n \left[\left|\cos \frac{\eta}{2}\right| + \left|\cos \frac{\eta'}{2}\right| \right] \tag{5}$$

The parameter ε_n appearing in the ion magnetic drift terms measures the toroidicity of the system, ε_c measures the connection length and S the shear. In slab geometry, these last two parameters always appear in the combination $\varepsilon_c S$, which is the shear parameter r_n/L_s (it should therefore be noted that ε_c is not really a measure of toroidicity). η_o is an arbitrary phase which can be regarded as specifying the centre of the perturbation and is related to the radial wavelength of the two-dimensional eigenmode, within a higher order theory [3]. For the most part we will assume $\eta_o = 0$, corresponding to modes centred on the outside of the minor cross-section of the torus.

In equation (1) the terms proportional to α arise from the $\underline{\nabla}B$ and curvature drifts of the ions. The integral term arises from the passing electron Landau resonance and is the appropriate asymptotic form [5] in the limits $\omega Rq/v_{Te} \ll 1$, $\frac{r}{R}\frac{M}{m}\cdot\frac{1}{\varepsilon_c S} \gg 1$ (otherwise the conventional slab result applies). If this term is omitted we are left with a Schröedinger equation, with an effective potential $U(\omega, \eta)$ which is in general complex. This is the eigenvalue equation solved in reference [3]. In the absence of toroidal curvature $(\alpha = \varepsilon_n = 0)$, the real part of the potential is a parabolic "anti-well". In this case the eigenfunctions will be propogating modes in η-space, which transform into the familiar shear damped outgoing-wave solutions of the plane slab. The effect of toroidal curvature is to introduce modulations into the effective potential which inhibit wave propagation. If the modulation is sufficiently strong it leads to the formation of local potential wells and "partially bound" eigenmodes.

Fig. 1 illustrates a plot of the potential function $U(\omega, \eta)$ with local potential wells in evidence centred on $\eta \simeq \pi/2$. Such a plot is typical of toroidal modes with $\eta_o = 0$. Potential wells such as these are associated with "partially bound" eigenmodes. Outward convection of energy occurs only through tunnelling leakages and is very small. These are the modes of reference [3] for which shear damping is negligibly small.

In this paper we will be concerned with establishing whether the electron Landau resonance is effective in destabilising these weakly damped eigenmodes.

3. NUMERICAL METHOD

We have solved equation (1) numerically, by expanding the perturbed potential $\phi(\eta)$ in a set of orthonormal basis functions:-

$$\phi(\eta) = \sum_{n=0}^{N-1} a_n \, h_n(\eta) \tag{6}$$

If the complex integro-differential operator on the left of equation (1) is denoted by $\mathcal{L}(\omega, \eta)$, operating with $\mathcal{L}$ on the expansion of ϕ, multiplying by $h_m(\eta)$ and integrating over all η generates a matrix eigenvalue equation

$$\sum_{n=0}^{N-1} a_n \, L_{mn}(\omega) = 0 \tag{7}$$

with

$$L_{mn}(\omega) = \int_{-\infty}^{\infty} d\eta \; h_m(\eta) \mathcal{L}(\omega, \eta) \; h_n(\eta) \,.$$

For even modes it is convenient to expand in even Hermite basis functions:-

$$h_n(\eta) = M_{2n}^{-\frac{1}{2}} \, H_{2n}(\sqrt{-i\sigma}\,\eta) \; e^{\frac{i\sigma\eta^2}{2}}$$

where H_p denotes a Hermite polynomial of degree p, $M_p = \sqrt{\frac{\pi}{-i\sigma}}\, 2^p\, p!$ and σ is an arbitrary complex parameter.

With the exception of the passing electron term, all the integrals involved in calculating the matrix elements L_{mn} can be evaluated analytically. The passing electron contribution is evaluated using a Gauss-Hermite quadrature scheme [6]. Since the frequency ω enters the operator $\mathcal{L}(\omega, \eta)$ in a complicated manner it is necessary to solve the matrix equation iteratively for ω. Thus the matrix equation is solved with an initial guess ω_o for the frequency. This yields an eigenvalue $\lambda(\omega)$ which is solved for ω to correct the initial guess. The iterations are repeated until convergence is obtained.

Up to 30 even basis functions can be retained in equation (6), though typically 15 gives adequate accuracy. With 15 basis functions a 48 point Gauss-Hermite scheme is used. The parameter σ is chosen to maximise the rate of decay of the amplitudes a_n with increasing n. The eigenvalue is then insensitive to variations of σ about this optimal value.

4. NUMERICAL RESULTS

The complex eigenfrequency ω of equation (1) has been calculated as an eigenvalue of the matrix equation (7) and can be considered as a function of the parameters η_o, ka_i, $\frac{rq'}{q}$, $\frac{r_n}{Rq}$, $\frac{r_n}{R}$, τ and η_e (η_o is a centreing parameter, ka_i is the effective wavenumber, $\frac{rq'}{q}$ is a measure of shear, $\frac{r_n}{Rq}$ is the ratio of density scale length to connection length, $\frac{r_n}{R}$ is a measure of field line curvature, τ is the ratio of electron to ion temperature and η_e the electron temperature gradient).

Our main interest is in the effects of toroidicity on the eigenvalue. These are discussed in section (a) and can be summarised as follows:-

As toroidal curvature (represented by r_n/R) is introduced into a slab-like system, there is a point at which shear induced damping becomes very weak. Then at a critical value of r_n/R the electron Landau resonance is able to drive the mode unstable, as is illustrated in figures 2 and 4.

In sections (b) to (d) we consider the effects of separately varying the parameters ka_i , η_e , $\frac{rq'}{q}$.

(a) The effect of varying toroidicity r_n/R

In this section we consider the effect we are principally interested in, that is the effect on the eigenvalue of the introduction of toroidal modulation into a slab-like system. The results are complicated by the fact that equation (1) admits multiple solutions in the presence of finite toroidicity. Thus additional eigenvalue branches appear at certain values of r_n/R (these are associated with the introduction of additional turning points into equation (1)) . Only one of these eigenvalue branches connects onto the slab eigenvalue.

In figure (2) we show plots of $\mathrm{Im}(\omega/\omega_*)$ against toroidicity r_n/R for three eigenvalue branches with $\eta_o = 0$, $ka_i = 0{\cdot}15$, $\frac{rq'}{q} = 1{\cdot}0$, $\frac{r_n}{Rq} = 0{\cdot}05$, $\tau = 1{\cdot}0$ and $\eta_e = 0{\cdot}0$. At $\frac{r_n}{R} = 0$ there is only one eigenvalue (see curve labelled "first harmonic") and this has the damping rate characteristic of the plane slab. As r_n/R is increased the damping is at first enhanced, due to increasing curvature of the central anti-well. As ε_n is increased further an off-centre potential well develops and this mode becomes "partially bound", only experiencing weak shear damping. Eventually the electron Landau resonance forces the mode into a weak instability.

However, for these particular parameters there is a more unstable eigenvalue branch (see curve labelled "fundamental"). This mode is driven strongly unstable for $\frac{r_n}{R} \gtrsim 0{\cdot}02$. There is also a third eigenmode, but this remains stable, because its real frequency is greater than unity and so the resonant electrons damp, rather than drive the mode.

Eigenfunctions for these three modes are illustrated in figure 3. It becomes clear why the mode labelled "first harmonic" is only weakly unstable, when it is realised that the driving term is roughly proportional to $\int_{-\infty}^{\infty} \phi(\eta) d\eta$. Inspection of figure 3 shows that there is a considerable degree of cancellation in the driving term for this particular mode.

It is always the case that the "fundamental" eigenmode (that with zero nodes of $\phi^*\phi$) is the most unstable. In the following we will concentrate our attention on this mode alone. It should be noted that there are parameters for which this most unstable eigenvalue branch connects smoothly onto the slab eigenvalue, as illustrated in figure 4. This shows $\text{Im}(\omega/\omega_*)$ plotted against r_n/R for such a case with $\eta_o = 0$, $ka_i = 0{\cdot}2$, $\frac{rq'}{q} = 0{\cdot}75$, $\frac{r_n}{Rq} = 0{\cdot}05$, $\tau = 1{\cdot}0$ and $\eta_e = 0{\cdot}0$. The initial enhancement of shear damping and the final instability are both very much in evidence.

For completeness we conclude this section with a discussion of the effect of toroidicity on modes centred on the inside of the minor cross-section of the torus $(\eta_o = \pi)$. Thus the broken curve in figure 2 illustrates the dependence of $\text{Im}(\omega/\omega_*)$ on r_n/R for such a mode. In this case the damping rate of the slab is hardly modified by toroidicity. This arises partly because of the shallowness of the central potential well (so that the shear damping is hardly modified) and partly because of favourable curvature on the inside of the torus. The latter effect causes an increase in real frequency which exceeds unity and results in damping from the electron Landau resonance. Thus as r_n/R is increased there is a gradual conversion from shear induced damping to electron Landau damping, with little change in the overall damping rate.

(b) <u>The effect of varying wavenumber ka_i</u>

In figures 5 and 6 we illustrate plots of $\mathrm{Re}(\omega/\omega_*)$ and $\mathrm{Im}(\omega/\omega_*)$ as functions of ka_i, with $\eta_o = 0$, $\frac{rq'}{q} = 1.0$, $\frac{r_n}{R} = 0{\cdot}06$, $q = 1{\cdot}2$, $\tau = 1{\cdot}0$ and $\eta_e = 0{\cdot}0$. The real frequency falls off almost linearly with increasing ka_i. This is a destabilising effect which may in part be responsible for the marked rise in the growth rate as ka_i is increased.

(c) <u>Electron temperature gradient η_e varying</u>

Figure 7 shows a graph of $\mathrm{Im}(\omega/\omega_*)$ as a function of electron temperature gradient η_e, for $\eta_o = 0$, $ka_i = 0{\cdot}15$, $\frac{rq'}{q} = 1{\cdot}0$, $\frac{r_n}{R} = 0{\cdot}06$, $q = 1{\cdot}2$ and $\tau = 1{\cdot}0$. The dependence of growth rate on η_e is linear. Positive electron temperature gradients (i.e. $\underline{\nabla T}_e$ in same direction as $\underline{\nabla n}$) are stabilising and negative temperature gradients destabilising. There is a critical value of η_e at which the mode is stabilised (corresponding approximately to $\frac{\omega_*}{\omega}(1 - \eta_e/2) - 1 = 0$). It is surprising that such long wavelength modes require quite substantial positive electron temperature gradients ($\eta_e \sim 1$) for stability.

(d) Shear varying

The effect of varying shear is illustrated in figures 8 and 9. These show plots of $\mathrm{Re}(\omega/\omega_*)$ and $\mathrm{Im}(\omega/\omega_*)$ against shear parameter $\frac{rq'}{q}$ with $\eta_o = 0$, $ka_i = 0{\cdot}1$, $\frac{r_n}{R} = 0{\cdot}06$, $q = 1{\cdot}2$, $\tau = 1{\cdot}0$ and $\eta_e = 0{\cdot}0$. For these parameters the growth rate peaks at a value of $\frac{rq'}{q}$ near 1·6. Thus for values of $\frac{rq'}{q}$ of interest to Tokamaks $\left(\frac{rq'}{q} \sim 1\right)$, increasing shear leads to an increasing growth rate. This is due in part to the destabilising downward shift in $\mathrm{Re}(\omega/\omega_*)$ as the shear is increased.

Finally in figures 10 and 11 we show similar plots of $\mathrm{Re}(\omega/\omega_*)$ and $\mathrm{Im}(\omega/\omega_*)$ against $\frac{rq'}{q}$ for $\eta_o = 0$, $ka_i = 0{\cdot}1$, $\frac{r_n}{R} = 0{\cdot}1$, $q = 1{\cdot}0$, $\tau = 10{\cdot}0$ and $\eta_e = 0{\cdot}0$. These parameters were chosen so as to make a detailed comparison between our numerical results and those of Chen and Cheng [7]. Our results are in good agreement with their perturbation treatment of the Ballooning equation (i.e. in η-space), but <u>not</u> with the eigenvalues obtained by exact numerical solution of the differential-difference equation in real space (i.e. x-space). It is not clear that the two methods of solution are entirely equivalent; the modes may have different radial structures.

5. CONCLUSION

The central result of this paper is the demonstration that toroidal effects can destabilise the slab drift wave. That is, the electron Landau resonance appropriate to toroidal geometry is indeed sufficient to overcome the residual shear damping characteristic of toroidal systems, which was previously discussed in [3].

Thus numerical solutions have been obtained for an eigenmode equation representing long wavelength drift modes in a tokamak, incorporating the passing electron Landau resonance, ion $\underline{\nabla B}$ and curvature drifts. Absolutely unstable eigenmodes have been found ballooning on the outside of the minor cross-section. In addition, the influence of a number of geometrical and other parameters on these waves have been investigated. In particular these appear to be destabilised by decreasing wavelength and increasing shear (up to a threshold at which increasing shear becomes stabilising). Positive electron temperature gradients are found to be stabilising, however stability is only achieved at moderately large values of η_e.

6. ACKNOWLEDGEMENTS

The author would like to acknowledge help from members of the Theory Division at Culham Laboratory, particularly Drs J.W. Connor, R.J. Hastie, J.B. Taylor FRS, and W.M. Tang (on attachment from Princeton Plasma Physics Laboratory).

7. REFERENCES

[1] ROSS, D.W., MAHAJAN, S.M., Phys. Rev. Lett. 40 (1978) 324.

[2] TSANG, K.T., CATTO, P.J., WHITSON, J.C., SMITH, J., Phys. Rev. Lett. 40 (1978) 327.

[3] HASTIE, R.J., HESKETH, K.W., TAYLOR, J.B., Nucl. Fusion 19 (1979) 1223.

[4] CONNOR, J.W., HASTIE, R.J., TAYLOR, J.B., Proc. Roy. Soc. A 365 (1979) 1.

[5] CONNOR, J.W., HASTIE, R.J., TAYLOR, J.B. To be published.

[6] STROUD, A.H., SECREST, D., Gaussian Quadrature Formulas (Prentice-Hall) (1966).

[7] CHENG, C.Z., CHEN, L., Princeton Plasma Physics Lab. Rep. PPPL-1579 (1979).

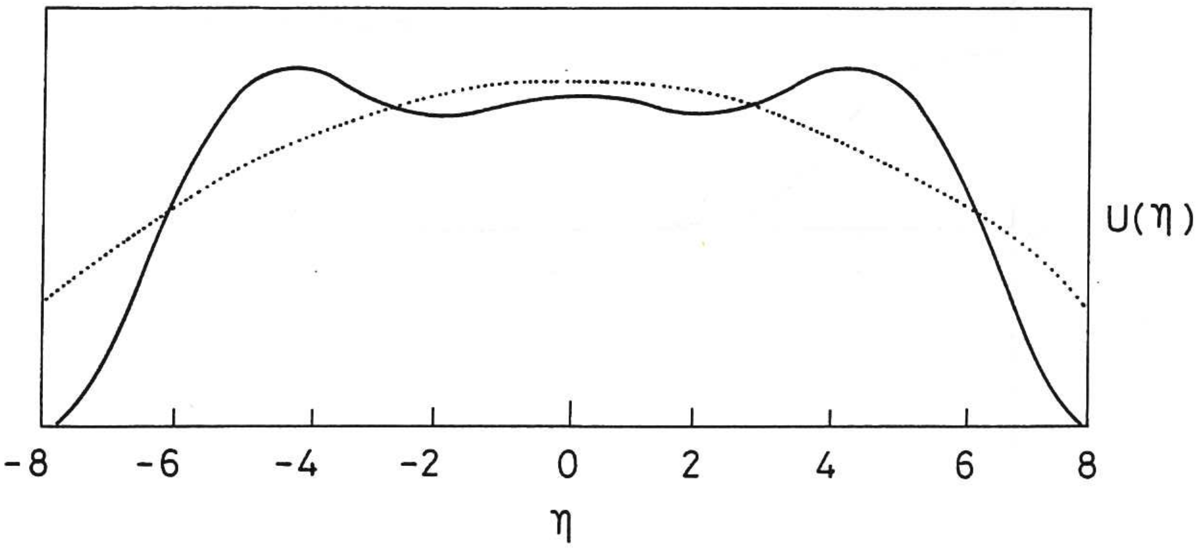

Fig.1 The potential function $U(\eta)$ for modes ballooning to the outside of the minor cross-section ($\eta_o = 0$). The broken curve is the corresponding "anti-well" potential of the slab.

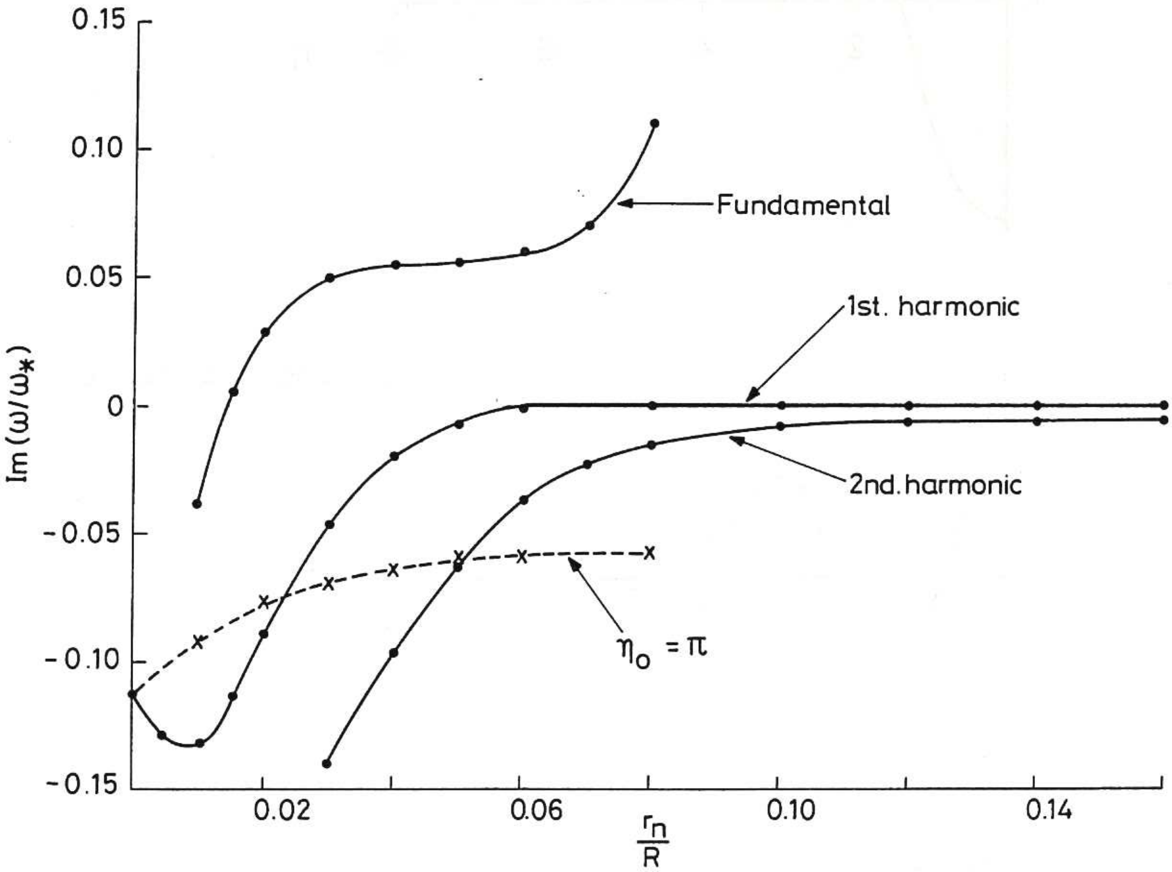

Fig.2 Full curves:- Plots of $\text{Im}(\omega/\omega_*)$ against toroidicity $\frac{r_n}{R}$ for three eigenmodes, with $\eta_o = 0$, $ka_i = 0{\cdot}15$, $\frac{rq'}{q} = 1{\cdot}0$, $\frac{r_n}{Rq} = 0{\cdot}05$, $\tau = 1{\cdot}0$ and $\eta_e = 0{\cdot}0$. Broken curve is for a mode ballooning to the inside of the minor cross-section ($\eta_o = \pi$).

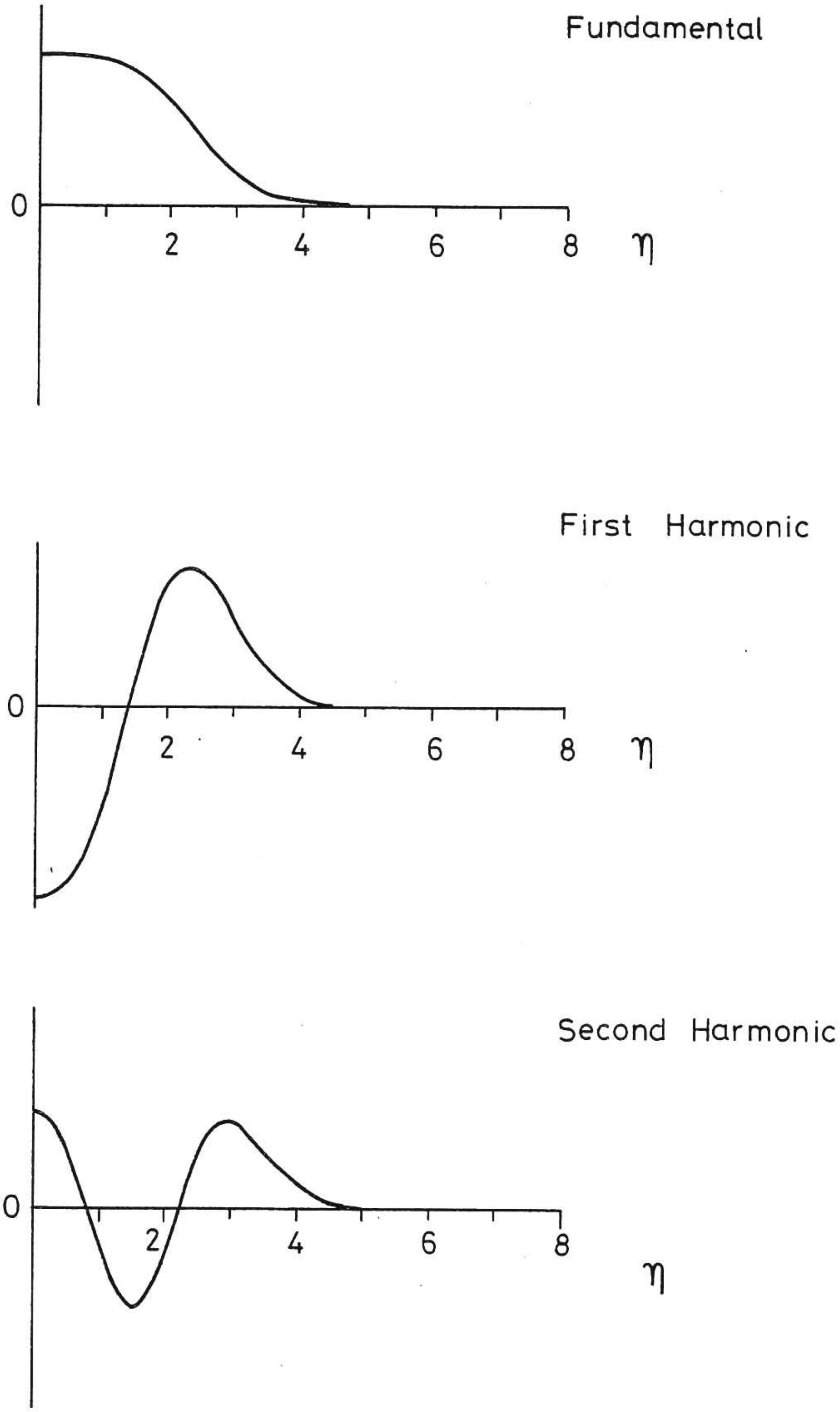

Fig.3 Eigenfunctions for $\eta_o = 0$, $ka_i = 0{\cdot}15$, $\frac{rq'}{q} = 1{\cdot}0$, $\frac{r_n}{Rq} = 0{\cdot}05$, $\tau = 1{\cdot}0$ and $\eta_e = 0{\cdot}0$.

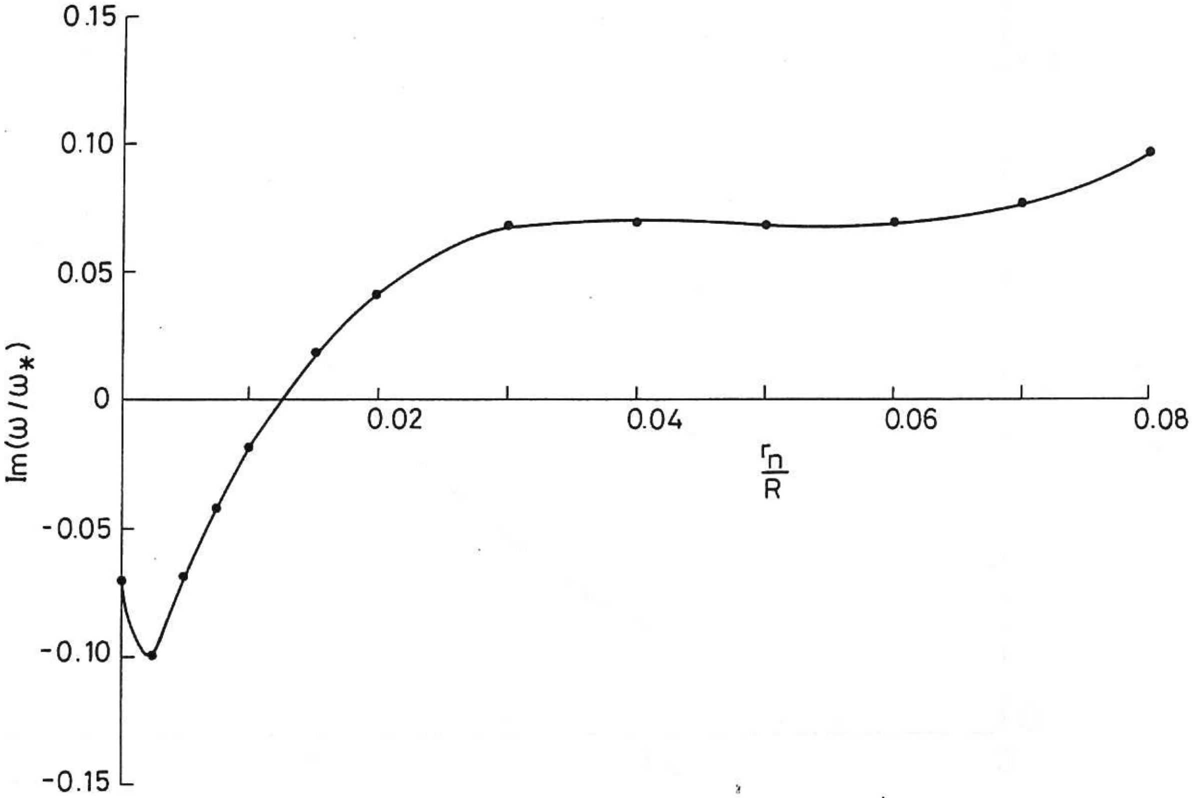

Fig.4 Plot of $\mathrm{Im}(\omega/\omega_*)$ against toroidicity $\frac{r_n}{R}$ with $\eta_o = 0$, $ka_i = 0{\cdot}2$, $\frac{rq'}{q} = 0{\cdot}75$, $\frac{r_n}{Rq} = 0{\cdot}05$, $\tau = 1{\cdot}0$ and $\eta_e = 0{\cdot}0$.

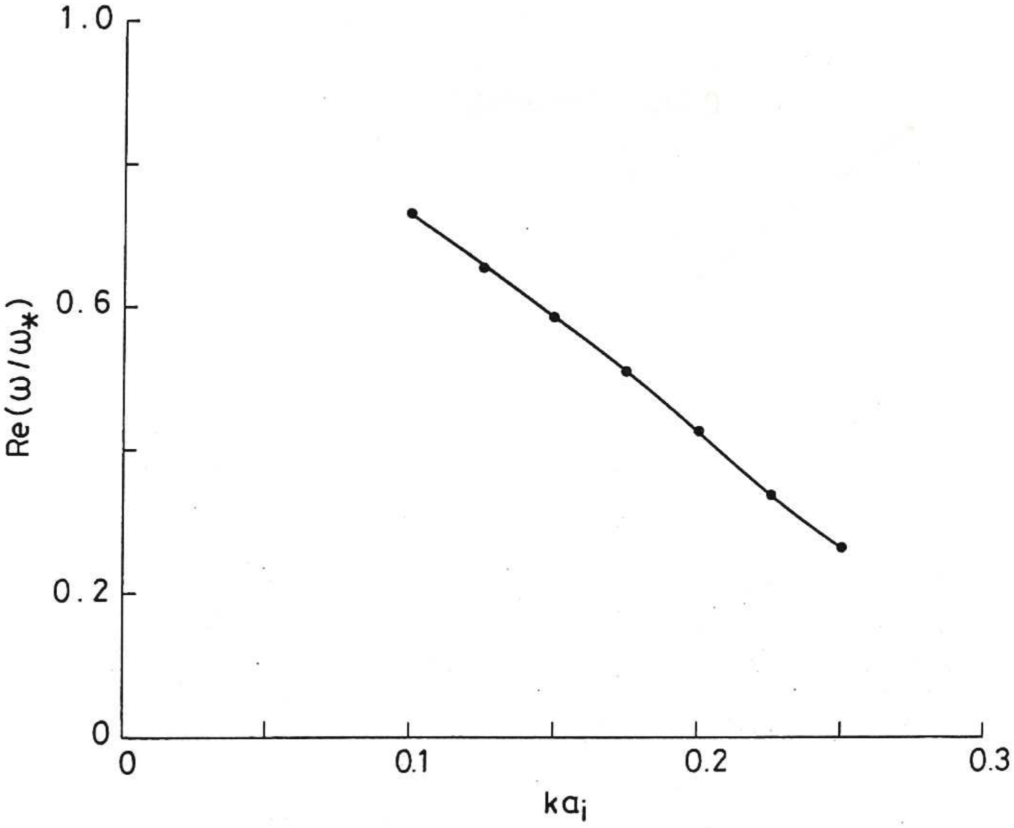

Fig.5 Dependence of $\mathrm{Re}(\omega/\omega_*)$ on wavenumber ka_i, with $\eta_o = 0$, $\frac{rq'}{q} = 1{\cdot}0$, $\frac{r_n}{R} = 0{\cdot}06$, $q = 1{\cdot}2$, $\tau = 1{\cdot}0$ and $\eta_e = 0{\cdot}0$.

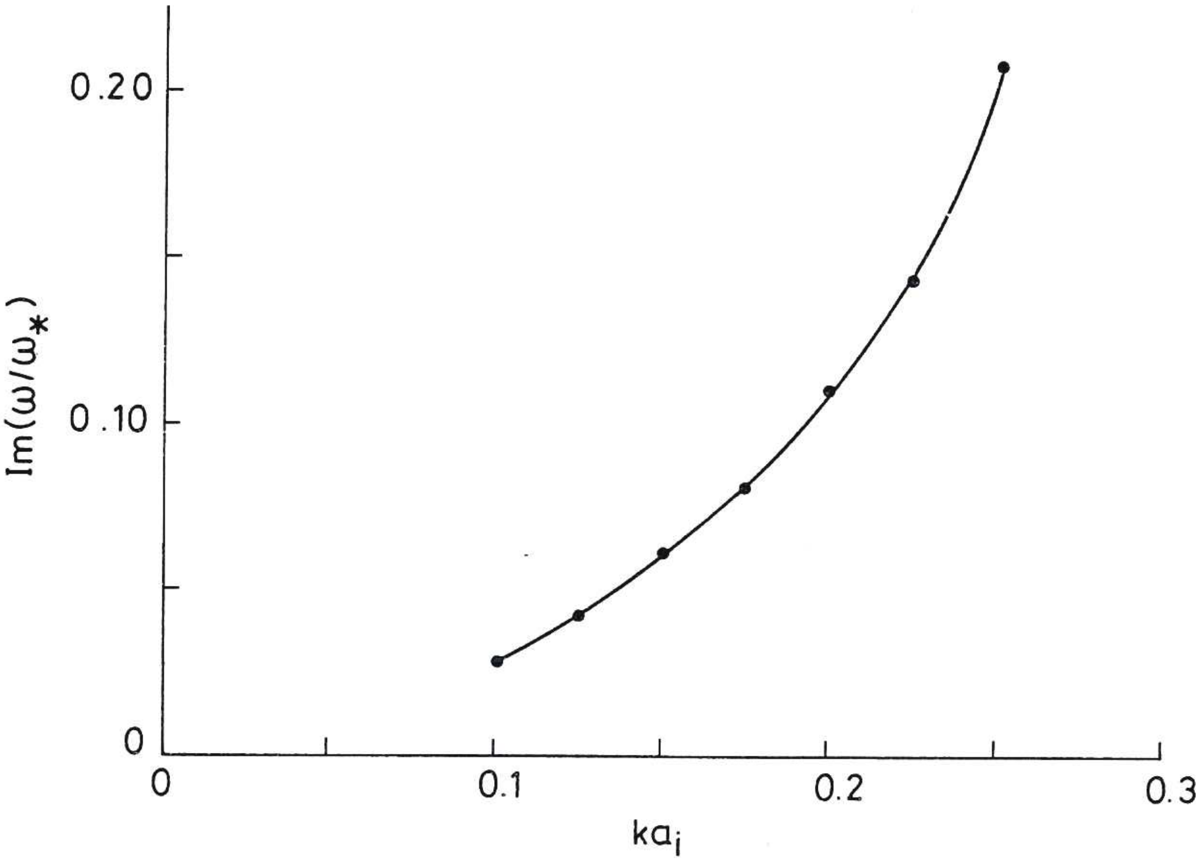

Fig.6 Dependence of Im(ω/ω_*) on wavenumber ka_i. Same parameters as Fig.5.

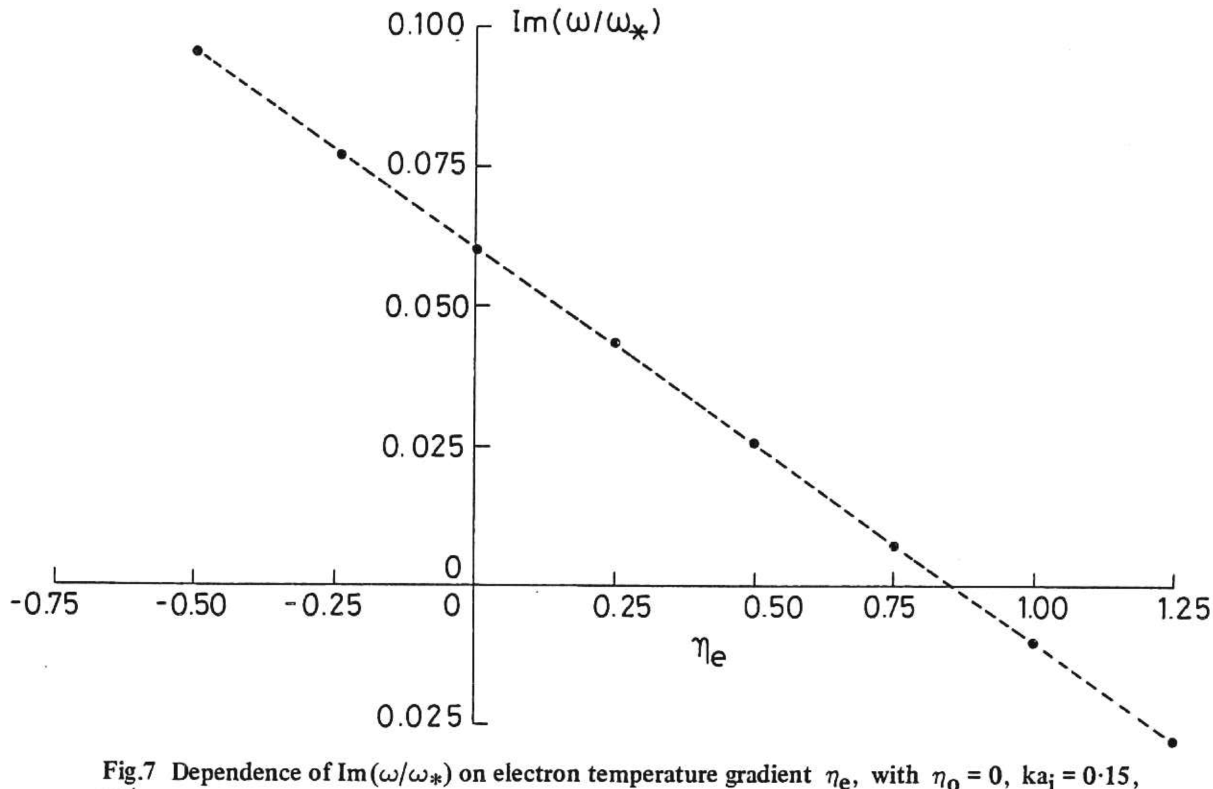

Fig.7 Dependence of Im(ω/ω_*) on electron temperature gradient η_e, with $\eta_o = 0$, $ka_i = 0{\cdot}15$, $\frac{rq'}{q} = 1{\cdot}0$, $\frac{r_n}{R} = 0{\cdot}06$, $q = 1{\cdot}2$ and $\tau = 1{\cdot}0$.

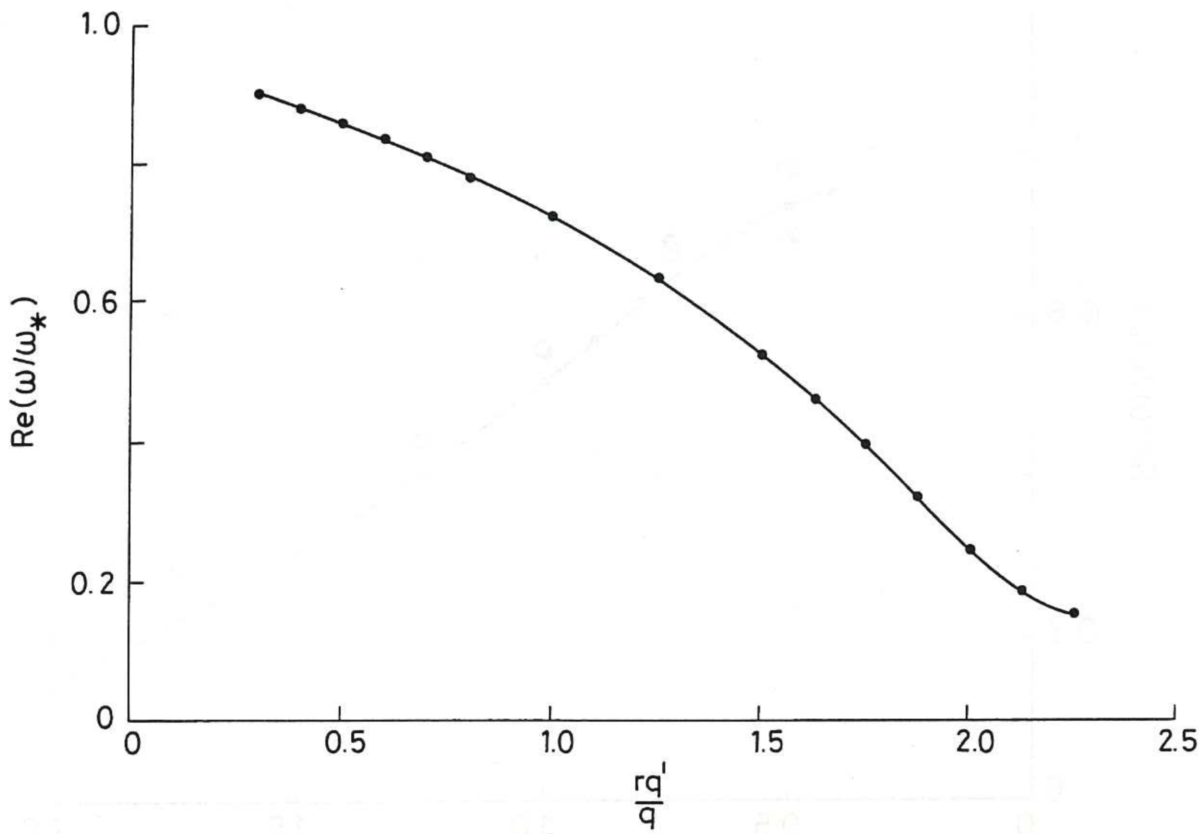

Fig.8 Dependence of $Re(\omega/\omega_*)$ on shear $\frac{rq'}{q}$ for $\eta_o = 0$, $ka_i = 1{\cdot}0$, $\frac{r_n}{R} = 0{\cdot}06$, $q = 1{\cdot}2$, $\tau = 1{\cdot}0$ and $\eta_e = 0{\cdot}0$.

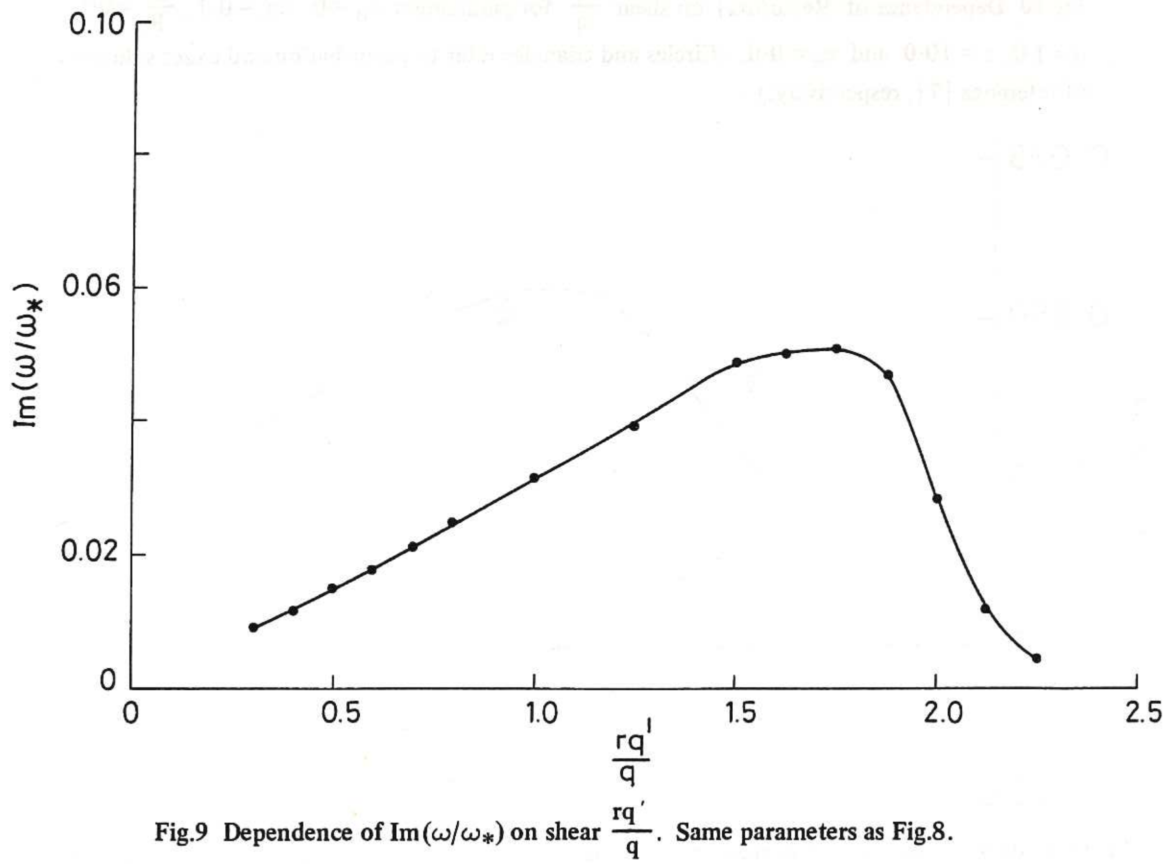

Fig.9 Dependence of $Im(\omega/\omega_*)$ on shear $\frac{rq'}{q}$. Same parameters as Fig.8.

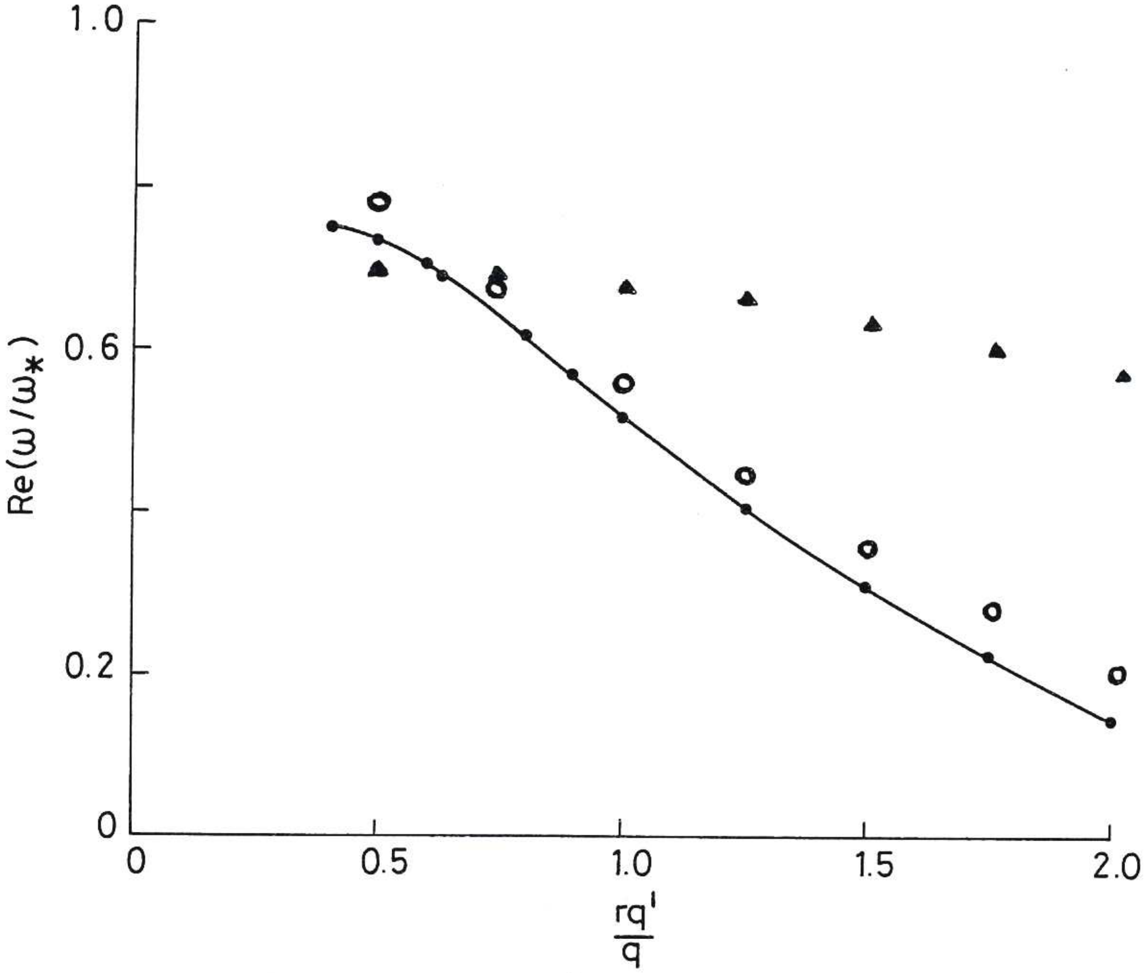

Fig.10 Dependence of $\mathrm{Re}(\omega/\omega_*)$ on shear $\frac{rq'}{q}$ for parameters $\eta_0 = 0$, $ka_i = 0{\cdot}1$, $\frac{r_n}{R} = 0{\cdot}1$, $q = 1{\cdot}0$, $\tau = 10{\cdot}0$ and $\eta_e = 0{\cdot}0$. (Circles and triangles refer to perturbation and exact solutions of reference [7], respectively.)

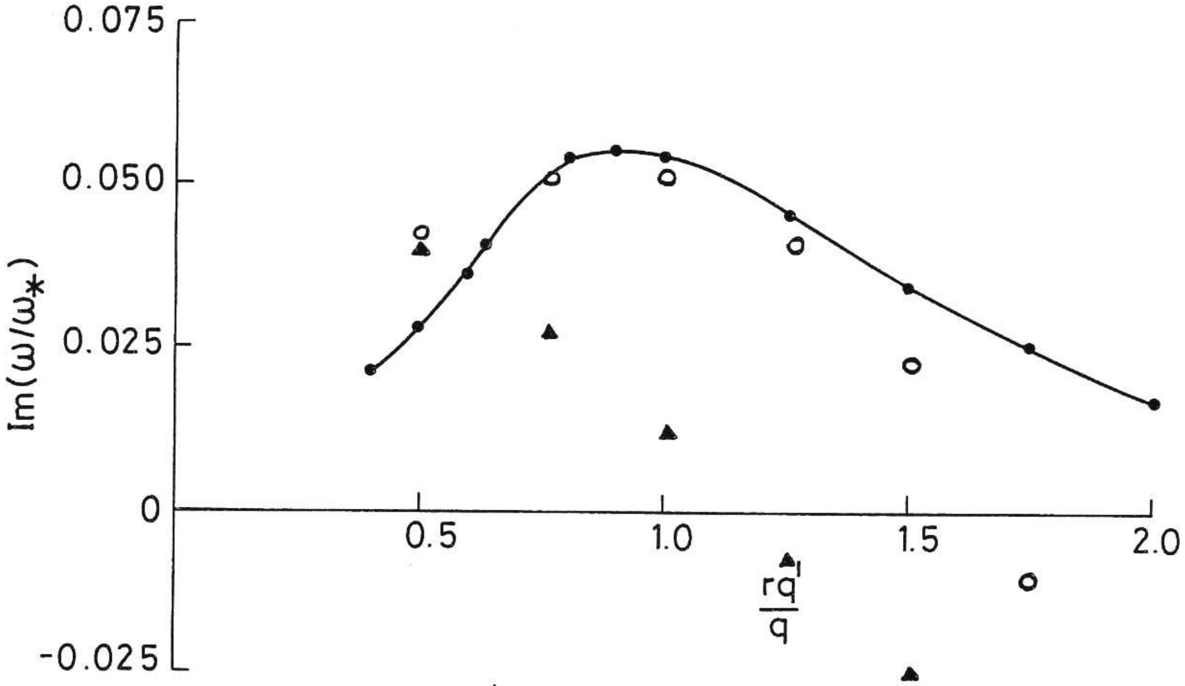

Fig.11 Dependence of $\mathrm{Im}(\omega/\omega_*)$ on shear $\frac{rq'}{q}$. Same parameters as Fig.10. (Circles and triangles refer to perturbation and exact solutions of reference [7], respectively.)